Bioconjugate Chemistry

Article

pubs.acs.org/bc

Differential Endosomal Pathways for Radically Modified Peptide Vectors

Piret Arukuusk,*[,†,‡] Ly Pärnaste,[†] Helerin Margus,[§] N. K. Jonas Eriksson,[‡] Luis Vasconcelos,[‡] Kärt Padari,[§] Margus Pooga,[§] and Ülo Langel[†,‡]

[†]Laboratory of Molecular Biotechnology, Institute of Technology, University of Tartu, Nooruse 1, 50411 Tartu, Estonia

[§]Department of Developmental Biology, Institute of Molecular and Cell Biology, University of Tartu, Riia 23, 51010 Tartu, Estonia

[‡]Department of Neurochemistry, The Arrhenius Laboratories for Natural Sciences, Stockholm University, SE-10691 Stockholm, Sweden

Supporting Information

ABSTRACT: In the current work we characterize the uptake mechanism of two NickFect family members, NF51 and NF1, related to the biological activity of transfected plasmid DNA (pDNA). Both vectors condense pDNA into small negatively charged nanoparticles that transfect HeLa cells with equally high efficacy and the delivery is mediated by SCARA3 and SCARA5 receptors. NF1 condenses DNA into less homogeneous and less stable nanoparticles than NF51. NF51/pDNA nanoparticles enter the cells via macropinocytosis, while NF1/pDNA complexes use clathrin- or caveolae-mediated endocytosis and macropinocytosis. Analysis of separated endosomal compartments uncovered lysomotropic properties of NF51 that was also proven by cotransfection with chloroquine. In summary we characterize how radical modifications in peptides, such as introducing a kink in the structure of NF51 or including extra negative charge by phospho-tyrosine substitution in NF1, resulted in equally high efficacy for gene delivery, although this efficacy is achieved by using differential transfection pathways.

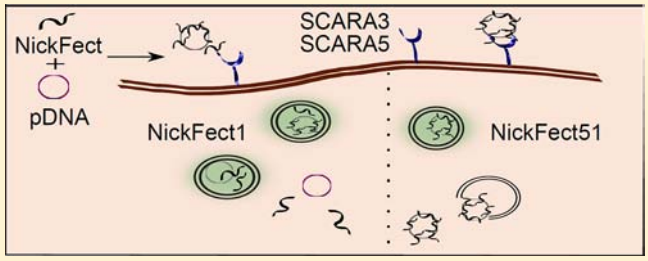

INTRODUCTION

Development of new drugs with increased specificity and lower side effects than currently used low molecular mass medications is of crucial significance for the treatment of devastating illnesses such as cancers or genetic disorders. Through rational design based on molecular, cellular, and structural data, macromolecules with protein modulatory functions can be developed to treat different diseases. Still, the clinical potential of large biomolecules remains poorly exploited due to their low bioavailability as the plasma membrane poses a formidable barrier to reach the target within the cells. Hence the success or failure of gene therapy critically relies on gene delivery, and the development of macromolecule-based drugs is dependent on the progress in the design of carrier molecules that can protect the cargo from degradation and facilitate their transfection.

To overcome the obstacles of gene intracellular delivery, numerous transfection techniques, both viral and nonviral, have been proposed. The safety concerns of viral vectors have hampered their utilization in clinics[1] and enhanced interest in nonviral delivery methods. The majority of nonviral delivery vectors are polycationic and are typically based on different lipids, polymers, or peptides that can neutralize pDNA charge and condense it into nanoparticles.[2,3] One group of nonviral vectors, cell-penetrating peptides (CPP), has been used for the intracellular delivery of a wide variety of biologically active cargos, such as plasmid DNA (pDNA), oligonucleotides, short interfering RNA (siRNA), both *in vitro* and *in vivo* without toxic side effects.[4−8] This corroborates the high potential of CPPs as carriers for therapeutics and several CPP based systems have reached clinical trials.[9,10]

Detailed knowledge about the cellular uptake and the intracellular fate of the delivered molecules is needed to avoid unwanted side effects and to facilitate the endosomal escape of the cargo *in vivo* applications.[11] These are prerequisites for the consecutive successful design of novel delivery vectors and macromolecules.

Even though the delivery properties of CPPs are undoubted, their uptake mechanism is still controversial. Relying on several studies about uptake mechanisms of CPP/cargo complexes, it has become more obvious that there is no universal pathway for cell entry, but the route depends on the physicochemical properties of the CPP and on the nature of the cargo molecule.[7,11−13] Broadly, there are at least two ways of entry: by endocytotic pathway or by direct penetration. CPPs mostly exploit an energy dependent internalization mechanism that first involves interaction with cellular membrane components, such as heparin sulfates or receptors, and thereafter entrance through different pathways of endocytosis, e.g., clathrin- or

Received: June 9, 2013
Revised: August 12, 2013
Published: August 28, 2013

dx.doi.org/10.1021/bc4002757 | *Bioconjugate Chem.* 2013, 24, 1721−1732

caveolae-mediated endocytosis, macropinocytosis.[14] For some CPP/cargo complexes direct penetration is considered the main route of entry.[15,16] As CPPs primarily utilize endocytotic pathways to enter the cells, CPP/cargo complexes reach endosomal compartments and are entrapped there. To overcome this major limitation, several strategies have been developed, e.g., addition of endosomotropic agents to the complex,[17] introduction of histidine-rich structures[18] or endosomolytic trifluoromethylquinoline motif,[19] and modifying the peptide with fatty acid.[20,21]

We have recently developed a new group of stearylated transportan 10 (TP10) analogs, named NickFect, that have proven to be highly efficient delivery vectors for pDNA, siRNA, and splice-correcting oligo (SCO) intracellular delivery.[22,23] Unraveling the internalization mechanism of these peptides is fundamental for their further development and use as carrier vectors both *in vitro* and *in vivo*. In the current work we are focused on a detailed characterization of the pDNA complexes and the uptake mechanisms of NickFect51 (NF51) and NickFect1 (NF1). These peptides have different chemical structure, but equally high transfection efficacy. Therefore we analyze the properties of peptide/cargo nanoparticles, internalization mechanism, and intracellular trafficking with regard to the biological activity of transfection.

EXPERIMENTAL PROCEDURES

Materials. All Fmoc-amino acids and activators for peptide synthesis were obtained from Iris Biotech GmbH, Germany. Solvents were purchased from Scharlau, Spain. siRNAs, Lipofectamine2000, and Lipofectamine RNAiMAX were purchased from Life Technologies, Sweden. All other chemical, including inhibitors and Percoll, were obtained from Sigma-Aldrich, Sweden.

Peptide Synthesis. NF1 and NF51 were synthesized and purified as described earlier[22,23] using fluorenylmethyloxycarbonyl (Fmoc) solid-phase peptide synthesis strategy. For carboxyfluorescein (FAM) labeled peptides, 5,6-carboxyfluorecein was coupled on-resin to α-NH_2 group of additional lysine in the C-terminus of peptides (Scheme S1).

Cell Culture. HeLa cells were grown in Dulbecco's modified Eagles medium (DMEM) supplemented with glutamax, 0.1 mM nonessential amino acids, 1.0 mM sodium pyruvate, 10% fetal bovine serum (FBS), 100 U/mL penicillin, and 100 μg/mL streptomycin (PAA Laboratories GmbH, Germany).

Complex Formation and Plasmid Transfection. HeLa cells (5×10^4) were seeded 24 h prior to experiment into 24-well plates. The luciferase expressing plasmid (pGL3), 4.7 kbp (Promega, Sweden) 1 μg/mL was mixed with NFs at different charge ratios of peptide over plasmid (CR 1−4) in Milli-Q H_2O in 1/10th of the final treatment volume and complexes were formed after 1 h incubation at room temperature. The medium on cells was replaced with fresh serum-containing medium before treatment with complexes. In SCARA inhibition experiments, the cells were incubated with specific inhibitor ligand (dextran sulfate, fucoidan, poly I) or control compound (chrondrotin sulfate, galactose, poly C) at concentration 1−5 μg/mL for 30 min prior to addition of preformed NF/pDNA nanocomplexes. In the experiments with endocytosis inhibitors, the cells were incubated with chloropromazine (10 μM), cytochalasin D (4 μM), or nystatin (50 μM) for 30 min before the addition of NF/pDNA nanocomplexes. Chloroquine at concentration of 100 μM was added to the cells directly prior to treatment with preformed NF/pDNA complexes. Cells were treated with NF/pDNA complexes for 4 h in serum-containing medium, thereafter the medium was replaced with fresh serum-containing medium in order to avoid toxic effects of the inhibitors and incubated for additional 20 h. Lipofectamine2000 was used according to the manufacturer's protocol. In experiments, assessing the impact of temperature on transfection efficacy, cells were kept for 30 min at 4 °C prior to addition of complexes and then treated at 4 °C for additional 4 h. Thereafter fresh medium was added and cells were cultivated at 37 °C for additional 20 h.

Before bioluminescence measurement, the cells were washed twice with phosphate buffered saline (PBS), lysed using 100 μL 0.1% Triton X-100 in PBS buffer for 30 min at 4 °C. Luciferase activity was measured in relative light units (RLU) using Promega's luciferase assay system on GLOMAX 96 microplate luminometer (Promega, Sweden). The data was normalized to protein content measured by DC protein determination kit (Bio-Rad Laboratories, Inc., USA).

siRNA Treatment. To downregulate scavenger receptors expressed in HeLa cells, SCARA3 and SCARA5 siRNAs were used as a mixture (25 nM of each). Scrambled siRNA was used at equal concentration (50 nM) as a negative control. The cells were transfected with siRNA using 1 μL/well Lipofectamine RNAiMAX for 4 h according to the manufacturer's protocol, followed by replacement of the medium with fresh medium to avoid toxic effects. NF/pDNA nanocomplexes were added 24 h post-transfection with siRNAs. Bioluminescence of luciferase was measured 24 h post-transfectionally of NF/pDNA nanocomplexes as described above.

DLS, Zeta-Potential Analysis, and Heparin Displacement Assay. Hydrodynamic mean diameter and ζ-potential of the nanocomplexes was determined by dynamic light scattering (DLS) studies using a Zetasizer Nano ZS apparatus (Malvern Instruments, United Kingdom). NF/pDNA complexes were prepared in Milli-Q H_2O according to the protocols for transfection and diluted in OptiMEM (Invitrogen, Sweden) with 10% fetal bovine serum. The pH was titrated using HCl solution. All results were based on three measurements from two independent samples. All data were converted to "relative by intensity" plots from where the mean hydrodynamic diameter was derived.

DNA condensation was analyzed by ethidium bromide (EtBr) exlusion assay. Heparin sodium was added to the preformed complexes over a range of concentrations from 0.5 to 10 mg of salt to 1 mL of complex solution and incubated at 37 °C for 30 min. Following the incubation period, loading buffer was added and samples were analyzed after being electrophoresed on agarose gel (1%) in TAE (0.5×) and imaged by staining in the gel with EtBr (0.5 μg/mL). For spectorfluorometry complexes were formed and treated with heparin as described above. Thereafter EtBr solution was added to give final concentration of 400 nM of EtBr per well. After 10 min of incubation at room temperature, fluorescence was measured on a Spectra Max Gemini XS fluorometer (Molecular Devices, Palo Alto, CA) at λ_{ex} = 518 nm and λ_{em} = 605 nm. Results are given as a relative fluorescence where value of 100% is attributed to the fluorescence of naked DNA in the same concentration as added to the complexes.

CD Spectroscopy. Circular dichroism (CD) spectra were recorded with a Applied Photophysics Chirascan (Applied Photophysics, Leatherhead, UK) using quartz cells of 0.1 cm optical path length. Scans were recorded at 37 °C between 185 and 260 nm with a 5 nm step resolution and 1 s per point from

20 μM solutions of NF1, NF51 peptides, or preformed complexes of NF with pGL3 plasmid (CR3) in Milli-Q H_2O. All spectra were corrected for background scattering by subtracting a solvent only spectrum. In order to obtain the spectra for peptides in the presence of pDNA, the circular dichroism signal from pDNA alone was subtracted from the complexes signal. Values of ellipticity were converted to mean residue ellipticity. To verify the exact concentration of the solutions UV absorbance was measured with a UV spectrophotometer V-560 (Jasco Inc., Easton, MD, USA). Molar concentrations of peptides were determined using a molar extinction coefficient of $\varepsilon 274 = 1404\ M^{-1}\ cm^{-1}$ for tyrosine.

Preparation of Double-Labeled pDNA Nanocomplexes with NF1 and NF51. For the visualization of plasmid DNA, pGL_3 plasmid was covalently tagged with CX-Rhodamine (CX-Rh) by using a Nucleic Acid Labeling Kit according to the manufacturer's protocol (Label IT Nucleic Acid Labeling Kit, CX-Rhodamine, Mirus Bio LLC, WI). Briefly, pGL plasmid was dissolved in Milli-Q H_2O at concentration of 0.5 mg/mL and then mixed with CX-Rh reagent dissolved in Reconstitution Solution at a ratio 1:1 (w:v), the reaction was performed at 37 °C for 2 h in Labeling Buffer A (1×). This ratio leads to the binding of approximately 100−200 CX-Rh molecules per one pDNA, which should be sufficient for detection by confocal microscopy. Thereafter, the labeled plasmid was separated from free CX-Rh by ethanol precipitation and dissolved in Milli-Q H_2O at concentration 0.5 mg/mL. The nanocomplexes of pDNA with NickFects were formed at the charge ratio 3, and the labeled molecules were used at concentrations that yielded an equal signal of both fluorochromes in complex. The concentrations of the constituents of nanocomplexes were 0.5 μg/mL pDNA, 0.5 μg/mL pDNA-CX-Rh, 1.6 μM NF1 or NF51, and 0.2 μM NF1-FAM or NF51-FAM. The complexes were formed in Milli-Q H_2O in 1/10 of volume used for the treatment of cells at room temperature for 1 h.

Analysis of the Cellular Uptake of Fluorescent pDNA Nanocomplexes by Confocal Laser Scanning Microscopy. HeLa cells were seeded into 8-well chambered coverglasses (Nalge Nunc International, NY) at concentration 10 000 cells/well, and grown in Iscovés Modified Dulbecco's Medium (IMDM) (Gibco, Invitrogen, UK) containing 10% FBS), 100 IU/mL penicillin, and 100 μg/mL streptomycin. After 2 days the medium was removed and cells were incubated with fluorescently labeled pDNA nanocomplexes with NF1 or NF51 diluted in complete IMDM at concentrations of 1 μg/mL and 1.8 μM, respectively, at 37 °C for 1 h. Thereafter, the medium with complexes was removed, cells were washed with medium, and fresh medium was added. Images of live cells were captured after 30 min and 2 h with Olympus Flow View FV1000 confocal laser scanning microscope (Olympus, Japan) using 60× oil-immersion objective and excitation at 488 nm (for FAM) or 594 (for CX-Rh). The system was run in a sequential scanning mode where only one laser was active at a time. The images were analyzed with Olympus FV1000 software FV10-ASW and processed with Adobe Photoshop CS4.

Separation of Endosomal Compartments. HeLa cells (1.5×10^6) were seeded on 10 cm culture dish 24 h prior to experiment in order to achieve confluency of 70−90%. Before treatment medium was removed, cells were washed with PBS, fresh medium was added, and cells were incubated at 37 °C, 5% CO_2 for 20 min before adding preformed NF/pDNA complexes. Cells were treated with complexes for 0.2−24 h time period.

For the analysis of pDNA trafficking in endosomal pathway, cells were treated with complexes for 1 h. Thereafter the used media was removed, cells were washed with PBS, and new media was added. Samples were taken after specified periods of time, named the chase period, washed with PBS, and trypsinated (trypsin supplemented with 1× EDTA, Gibco, Life Technologies, USA) to detach the cells from the culture dish and to remove complexes associated with the cells. From this step all procedures were performed at 4 °C.

After trypsination cold PBS was added and the cells were centrifuged to achieve a soft pellet. The pellet was resuspended in 1.5 mL hypertonic buffer (3 mM imidazole, 0.25 M sucrose, and 1 mM EDTA in Milli-Q H_2O, pH 7.4), centrifuged and resuspended again before disruption of plasma membrane using 26G needle and a syringe (Terumo, Belgium). The resulting suspension was centrifuged to remove unbroken cells and larger membrane fragments. Supernatant was mixed with 6.7 mL balancing buffer, 2.2 mL 90% Percoll solution in 2.5 M sucrose and 0.2 mL 20% bovine serum albumin (BSA) and loaded to 2.5 M sucrose layer in ultracentrifuge tube (Beckman Coulter, USA), following centrifugation at 4 °C, 22 000g in vacuum (Beckman Optima LE-80K, SW41 Ti rotor) for 2 h to allow the gradient formation and organelles to reach isopycnic area. Thereafter, fractions were collected and DNA was precipitated with isopropanol LiCl mixture and ice-cold ethanol followed by incubation at 4 °C and at −20 °C for 1 h, respectively, and centrifugation for 30 min at 14 000 rpm. The pellet was dried at room temperature for 45 min and resuspended in 20 μL of Milli-Q H_2O. To detect intact NF/pGL3 complexes each fraction was analyzed on 2% agarose gel prior precipitation.

From precipitated samples PCR was used to amplify pGL3 giving a product of 142 basepairs. To DNA Milli-Q H_2O, reverse and forward primer (Microsynth, Switzerland) and 5× FIREPol Master Mix (Solis BioDyne, Estonia) containing 12.5 mM $MgCl_2$ were added. Samples were loaded on the gel and after 1.5 h of electrophoresis fluorescent DNA gel bands were detected using Typhoon gel scanner (GE Healthcare, UK). The baseline was corrected to fractions from untreated cells. Calibration curve was used to normalize results of fluorescence measurement.

Labeling of pDNA for Electron Microscopy. To visualize pDNA in cells by transmission electron microscopy, pGL3 plasmid was tagged with biotin and complexed with neutravidin-gold (NA-gold) conjugate (10 nm in diameter) (homemade).[24] Biotin was covalently coupled to pDNA by using Nucleic Acid Labeling Kit according to manufacturer's protocol (*Label* IT Nucleic Acid Labeling Kit, Biotin, Mirus Bio, USA). Briefly, the biotin reagent dissolved in Reconstitution Solution was mixed with pDNA (1 μg/μL) at a ratio 1:5 (v:v) in Labeling Buffer A for 1 h at 37 °C. The labeled plasmid was separated from free biotin by ethanol precipitation and dissolved in Milli-Q H_2O. Biotinylated pDNA (2 μg/mL) was first associated with NA-gold conjugate at 0.64 nM concentration for 30 min at 37 °C followed by complexation with NF51 or NF1 at CR3 in Milli-Q H_2O in 100 μL (1/10th of the final treatment volume) for 30 min at room temperature.

Treatment of Cells for Electron Microscopy. HeLa cells were seeded onto glass coverslips in 35-mm Petri dishes, grown to 80−90% confluency and incubated with full culture medium containing pDNA-NA-gold complexes with NF51 or NF1 for 1 to 4 h at 37 °C. After incubation, the coverslips with cells were

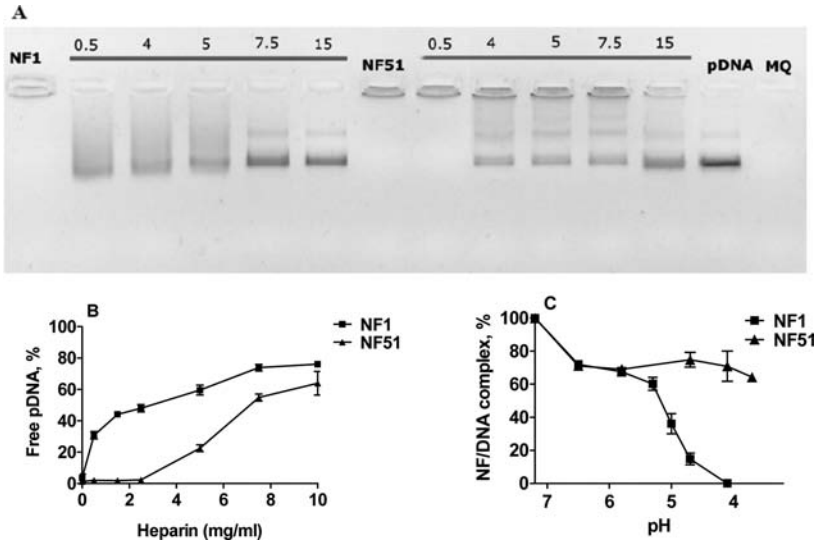

Figure 1. Physiochemical characterization of the NF/pDNA nanoparticles. (A) Comparison of the stability and the dissociation profile of NF1/pDNA and NF51/pDNA nanoparticles at CR3 upon treatment with heparin at different concentrations ranging from 0.5 to 15 mg/mL, analyzed by gel retardation assay. (B) Displacement of pDNA from NF/pDNA nanoparticles with heparin at different concentrations ranging from 0.5 to 10 mg/mL was analyzed by spectrofluorimetry. (C) Dissociation of NF/pDNA complex at acidic pH. The preformed complexes in MQ water were titrated with HCl to achieve different pH values and nanoparticle hydrodynamic diameter was measured by DLS. Nanoparticles at physiological pH were taken as 100%. Percentage of intact NF/pDNA nanoparticles was calculated according to the intensity of the peak.

placed into 24-well plates, washed, and fixed with 2.5% glutaraldehyde in cacodylate buffer (pH 7.4) for 1 h at room temperature. The cells were postfixed with osmium tetroxide and dehydrated with ethanol. The specimens were embedded in epoxy resin (TAAB Laboratories Equipment Ltd., UK), cut into ultrathin sections, and contrasted with uranyl acetate and lead citrate. The sections were examined with Tecnai G2 Spirit (FEI, Eindhoven, Netherlands) transmission electron microscope and microphotos were analyzed and processed with Adobe Photoshop CS4 software.

Statistics. Values in all experiments are represented as mean ± SEM of at least 3 independent experiments performed in duplicate. Differences were considered significant at $*p < 0.05$ using two-tailed Student's t test.

RESULTS

Characterization of NickFect/pDNA Complexes. The chemical structures of NickFect1 and NickFect51, recently designed in our group,[22,23] are presented in Scheme S1. NF1 contains a phosphorylated tyrosine in the third position and Ile11 is replaced with threonine as compared to stearylated TP10 sequence. In NF51 Lys7 is replaced with ornithine and the δ-amino group of ornithine is used for the subsequent synthesis instead of ordinarily used α-NH_2 group in order to gain a kinked structure.

The size of the nanoparticles is known to substantially affect their pharmacokinetics and pharmacodynamics[25] and the optimal in vivo uptake of such complexes is achieved in the case of <200 nm size.[26] DLS analysis revealed (Table S1) that complex formation of NF51 and NF1 with pDNA in water yields small nanoparticles with 60 nm diameter and positive ζ-potential (31 to 38 mV) for NF51 and negative ζ-potential (−18 to −13 mV) for NF1. The size of the particles remained in the same range at the both charge ratios 2 and 3 (peptide over plasmid). To mimic the physiological conditions, we added serum-containing medium to the nanoparticles preformed in water and measured the size and surface charge of resulting complexes. The presence of serum-containing medium quickly enlarged the size of NF/pDNA complexes from 60 to 160 nm and reverted the ζ-potential of both NF51 and NF1 complexes with pDNA to negative (−9 to 11 mV). During 1 h of incubation time the size of the nanoparticles increased gradually up to 405 or 480 nm for NF51 and NF1 complexes, respectively (Figure S1 C), suggesting the interaction and coating of nanoparticles with salts and serum proteins. Nevertheless, the complexes remained stable in the presence of serum and retained their negative surface charge.

CD spectra measurement of NickFect solutions in water revealed that applied modifications in the chemical structure of the peptides did not result in a detectable change in their helicity as the CD curves of NF51 and NF1 were practically indistinguishable (Figure S1 A, B). Spectra display characteristic features of an α-helical structure: minima at 222 and 208 nm and maximum at around 190 nm. Next, spectra for preformed NF/pDNA complexes were obtained. pDNA signal was subtracted from the complex signal, giving the signal of the individual peptides in the presence of the plasmid. The curves for the complexes no longer fitted a typical α-helical profile, the characteristic minima had disappeared (208 nm) or shifted (222 to 228 nm), and the maxima also shifted (190 to 195 for NF51/pDNA and 196 nm for NF1/pDNA). We can speculate that both spectra profiles are closer to one characteristic of a β-sheet or a mixture of α-helical and β-sheet conformation. These results show that, in the presence of the pDNA, both peptides change from an α-helical secondary structure to a different conformation, which cannot be clearly attained from the spectra, once they present noncanonical features attributed both to α-helical and β-sheet conformation.

The ideal carriers are peptides/polymers that not only protect and stabilize DNA but also allow pDNA unpacking, necessary for gene expression.[27] The transport vector should condense pDNA into stable nanoparticle and pDNA must be at least partially released from the complex once delivered into the cells. To characterize the ability of NF/pDNA complexes to

dx.doi.org/10.1021/bc4002757 | Bioconjugate Chem. 2013, 24, 1721−1732

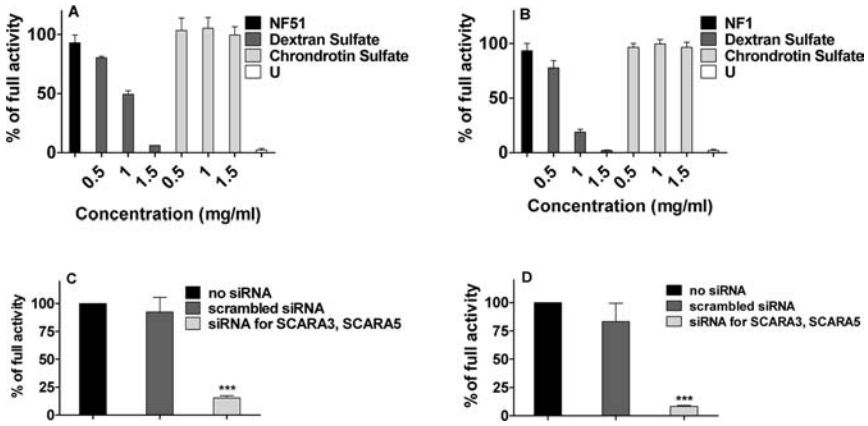

Figure 2. Scavenger receptors participate in NF/pDNA complex uptake into HeLa cells. Suppression of (A) NF51 and (B) NF1 mediated pDNA transfection in the presence of SCARA inhibitory ligand dextran sulfate. HeLa cells were incubated with dextran sulfate or negative control compound chrondrotin sulfate for 30 min prior to treatment with preformed NF/pDNA complexes. Transfected cells without pretreatment were taken as 100% and used as a positive control; untreated cells were used as a negative control. Downregulation of SCARA3 and SCARA 5 receptors inhibits pDNA transfection by (C) NF51- and (D) NF1. SCARA3 and SCARA5 were knocked down by siRNA 24 h before NF/pDNA transfection. Scrambled siRNA was used as a negative control. NF/pDNA transfection efficiency was assessed 24 h post-transfectionally. Results are presented as percentage of full activity of NF/pDNA nanocomplexes without pretreatment.

release the cargo we treated the preformed complexes with varying amounts of competitor molecule heparin and analyzed complex dissociation by using agarose gel electrophoresis. Interestingly, NF51/pDNA complexes were much more resistant to the treatment with heparin compared to NF1/pDNA complexes (Figure 1A). This was also confirmed by measuring spectrofluorimetrically the amount of liberated pDNA (Figure 1B). 2.5 mg/mL of heparin was needed to displace 50% of pDNA from NF1/pDNA complex while more than 7 mg/mL of heparin was required to achieve the same level of replacement in NF51/pDNA complex.

To assess the impact of acidic conditions to the stability of the complexes, we monitored the amount of intact NF/pDNA nanoparticles as a function of pH. Gradually increasing amount of HCl was added to preformed complexes in water, and hydrodynamic diameter of the complex was measured by DLS. Tracing the percentage of intact NF/pDNA complexes by relative intensity showed that NF1 complexes were less stable to the drop of pH. At pH 4.0 no entire NF1/pDNA nanoparticles were detected, while 64% of NF51/pDNA complexes remained unimpaired even at pH 3.7 (Figure 1C).

Scavenger Receptors Are Involved in pDNA Delivery by NF1 and NF51. To assess the biological activity of NF1 and NF51 nanoparticles with pDNA we complexed these peptides with luciferase-encoding plasmid (pGL3) and measured luciferase expression 24 h after transfecting HeLa cells with these nanoparticles. Both peptides efficiently mediated pDNA delivery into HeLa cells in the presence of serum proteins yielding gene expression levels more than 4 orders of magnitude higher than the background and almost reaching the transfection efficacy of commercial transfection reagent Lipofectamine2000 (Figure S2). Interestingly, despite the structural differences of NF51 and NF1, their efficacy to mediate gene delivery was similar.

We have recently shown that the uptake of pDNA complexes with stearylated TP10 analog PF14 is mediated by class A scavenger receptors (SCARAs).[28] As NF/pDNA complexes acquired negative ζ-potential in serum-containing medium, we aimed to assess if SCARAs are involved in the uptake of NF/pDNA nanocomplexes. We tested the effect of well-known specific inhibitory ligands for SCARA[29,30] polyinosinic acid (poly I), fucoidan, and dextran sulfate on the pDNA transfection activity mediated by NickFects. Structurally similar compounds poly C, galactose, and chrondroitin sulfate that lack affinity to SCARA were utilized as negative controls. The preincubation of cells with specific SCARA inhibitory ligands diminished gene delivery to 10% in a dose-dependent manner (Figure 2A,B; Figure S3). Dextran sulfate inhibited pDNA transfection mediated by NF51 and NF1 more than 90% already at a concentration of 1.5 μg/mL, while chrondroitin sulfate had no effect on transfection. Fucoidin (1.5 μg/mL) resulted in 90% inhibition of luciferase expression and poly I (5 μg/mL) inhibited 80% of pGL3 plasmid transfection mediated by NF1 and 50% in the case of NF51. The respective negative controls, galactose and poly C, had no effect on transfection. This data confirms the high impact of scavenger receptors in NF/pDNA complex uptake.

Our earlier studies demonstrated that precisely scavenger receptors from class A, SCARA3 and SCARA5, are involved in the uptake of PF14-SCO nanocomplexes.[31] To gain knowledge on the role of SCARA3 and SCARA5 in NickFect-mediated pDNA transfection we used siRNAs to knock down the two above-mentioned receptor subtypes. Pretreatment of HeLa cells with SCARA3 and SCARA5 siRNA (25 nM of each) yielded $\geq$85% inhibition of plasmid transfection with both NF51 and NF1 (Figure 2C,D) while the treatment with scrambled siRNA had no effect on transfection efficacy. These data strongly suggest the participation of SCARA3 and SCARA5 receptors in the transfection of NF/pDNA nanoparticles.

Interaction of Nanocomplexes with the Plasma Membrane and Their Intracellular Trafficking. In order to analyze the integrity of NF/pDNA nanoparticles during cellular uptake and intracellular trafficking, we produced double-labeled complexes where the peptide and plasmid DNA were tagged with different fluorochromes. This technique allowed us to track their uptake in real time using confocal laser scanning microscopy. In order to detect the rearrangement of nanoparticles we optimized their composition to yield an equal signal of each fluorochrome in complex, which displays complexes in a yellow color in combined image (Figure 3

dx.doi.org/10.1021/bc4002757 | Bioconjugate Chem. 2013, 24, 1721−1732

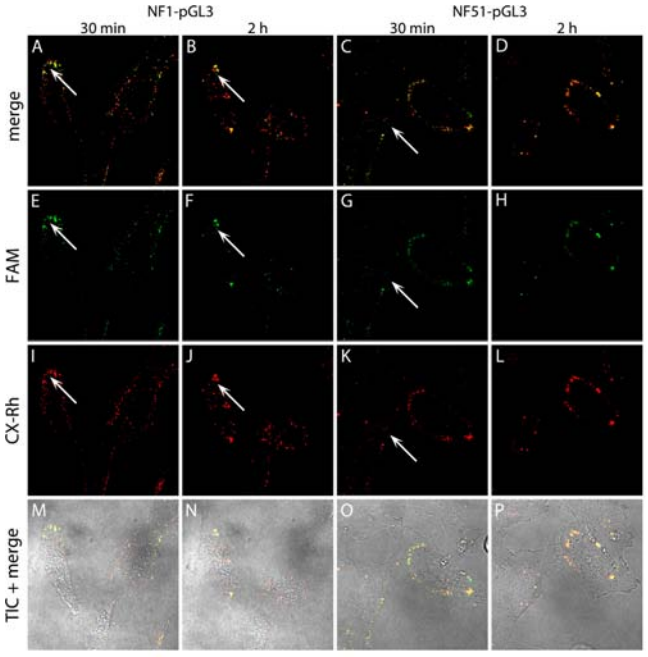

Figure 3. Internalization and intracellular trafficking of CX-Rh-labeled pDNA complexes with FAM-NF51 and FAM-NF1. HeLa cells were incubated with the complexes of CX-Rh-labeled pDNA and FAM-NF51 or FAM-NF1. The images of live cells were captured after 30 min and 2 h of incubation by confocal microscopy. The arrows indicate the presence of peptide that is not colocalized with pDNA.

upper and lower panel). Dissociation of NF that is labeled with green emitting fluorescence shifted the color of complexes from yellow to orange or red, whereas the exit of plasmid that emits red light makes the complex fluorescence more green than yellow. The NF1 and NF51 complexes with pDNA associated with the cell surface quickly, and in 15 min, the prominent labeling of cells had already taken place. However, the color of different NickFect complexes was remarkably different. Whereas the NF51/pDNA complexes associated with cells were predominantly yellow, the NF1/pDNA complexes were much more diverse and their signal was more often biased toward red or green (Figure 3A-D), probably because of peptide properties. NF51 seems to have the tendency to form more homogeneous population of complexes compared to NF1. On the surfaces of the cells, both NF1/pDNA and NF51/pDNA complexes also assembled into large conglomerates, which could reach even 2−3 μm in size (data not shown). In order to assess whether the aggregates formed before or after the association with the plasma membrane, we traced the fluorescently labeled NF/pDNA complexes in cell-free system using the total internal reflection fluorescence microscopy (TIRF) and in serum-containing cell-growth medium, but did not detect any conglomerates (data not shown). This indicates that NF/pDNA aggregates formed at the cell surface after the binding of the complexes to the plasma membrane. However, the formation of aggregates at the plasma membrane was still rather rare. Interestingly, in the case of both peptides we detected a fraction of peptide bound to the plasma membrane that was not associated with pDNA or complexes (Figure 3, arrows). The free peptide was distributed over the plasma membrane and was not localized close to NF/pDNA complexes. It has been speculated that in the case of noncovalent peptide-cargo complexes a fraction of peptide is not incorporated in the nanocomplexes and might act on its own. However, to our knowledge, this is the first study to demonstrate that the carrier peptide not involved in complexes associates with cells individually. After 30 min of incubation the majority of the NF/pDNA complexes resided at the cell periphery and had mainly yellowish color suggesting that the nanocomplexes did not reorganize upon association with extracellular matrix or recognition by receptors.[31] Later, after 2 h of incubation, however, the complexes shifted toward the perinuclear region and localized inside endosomal vesicles. Importantly, NF51/pDNA complexes retained their yellowish color even after 2 h of incubation, whereas NF1/pDNA complexes turned red. The more prominent shift of NF1/pDNA complexes to red color was probably caused by the maturation of early endosomes into late endosomes where the pH drop to 5−6 drastically decreased the green emission of fluoresceine. However, we cannot exclude that the loss of green fluorescence signal is caused by the partial dissociation of NF1 from complex with pDNA. These observations imply that NF51/pDNA complexes might exploit endosomal pathways in which vesicles are kept near-neutral,[32] or the complexes interfere with the acidification of endosomes. The NF1/pDNA complexes, in contrary, seemed to harness more clathrin-dependent endocytic pathways where the endosomes are quickly acidified and cargo molecules destined to degradation in lysosomes.

NF1 and NF51 Use Different Endocytotic Pathways for pDNA Delivery. A common way to assess the involvement of endocytosis is the treatment of cells with peptide/cargo complexes at lowered temperature that inhibits all energy-dependent pathways.[33] Incubating the cells at 4 °C during NF/pDNA transfection significantly decreased gene delivery efficacy (Figure S4), referring to energy-dependent uptake mechanism like endocytosis.

To further ensure the involvement of endocytic vesicles in the uptake, we transfected HeLa cells with NF/pDNA complexes in the presence of the well-known endosomolytic agent chloroquine (CQ). Surprisingly the presence of CQ only slightly increased the efficacy of gene delivery mediated by NF51, while it elevated NF1 mediated pDNA transfection more than 3-fold (Figure 4A). This indicates that although endocytic vesicles are involved in the uptake of both NF/pDNA and NF1/pDNA nanocomplexes, the complexes of NF51 and NF1 probably exploit different endocytic pathways. These data also suggest better escape of NF51/pDNA nanoparticles from endosomal compartments.

An extensively used method to pinpoint the particular endocytic pathways is by application of pharmaceutical endocytosis inhibitors that block a certain internalization route. Before transfection we pretreated the cells for 30 min with chloropromazine to inhibit clathrin-mediated endocytosis, with cytochalasine D known to suppress macropinocytosis or with nystatin for caveolin associated process. Gene delivery efficacy was measured and normalized with the control experiment in the absence of inhibitors. Cytochalasine D reduced NF51 mediated pDNA delivery to 25%, while chloropromazine and nystatin had no effect on transfection efficacy (Figure 4B) suggesting that NF51/pDNA nanoparticles are internalized via macropinocytosis. NF1 mediated gene delivery was reduced by 50% both in the presence of chloropromazine and cytochalasine D (Figure 4C) and by 20% with nystatin suggesting that NF1/pDNA nanoparticles

dx.doi.org/10.1021/bc4002757 | Bioconjugate Chem. 2013, 24, 1721−1732

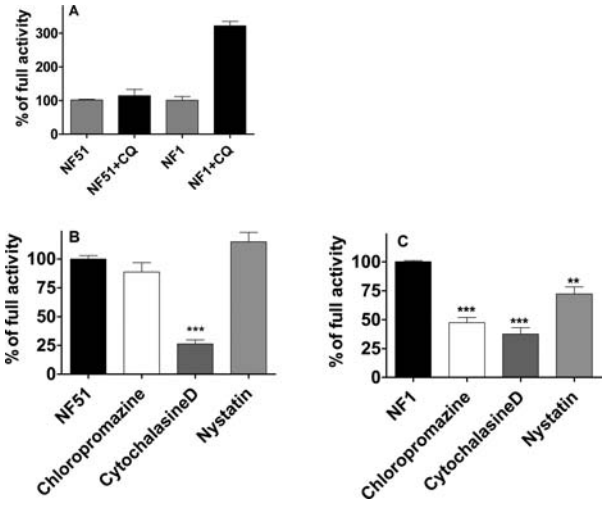

Figure 4. Effect of lysomotropic agent chloroquine (A) and endocytosis inhibitors (B, C) on NF51 and NF1 mediated gene delivery. (A) Chloroquine, CQ (100 μM) was added to HeLa cells directly prior to the treatment with preformed NF/pDNA complexes and biological activity was measured 24 h after transfection. (B, C) Endocytosis inhibitors chloropromazine (10 μM), cytochalasin D (4 μM), and nystatin (50 μM) were added 30 min before the addition of NF/pDNA complexes. Results are presented as percentage of full activity of NF/pDNA nanocomplexes without pretreatment.

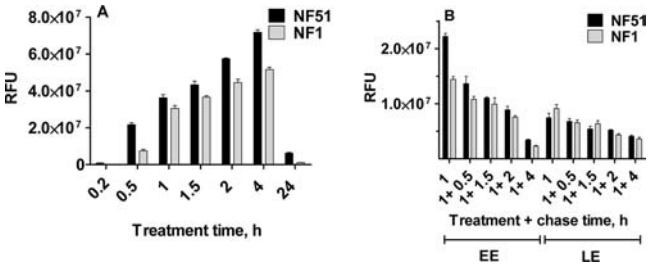

Figure 5. Uptake of NF/pGL3 complexes by HeLa cells and localization to endosomal comparments. (A) Uptake of NF/pGL3 complexes to endosomal compartments and release into cytosol. Cells were treated with NF/pGL3 complexes for 0.2−24 h. The pGL3 Luc gene was amplified with PCR and detected on 1% agarose gel. Relative fluorescence was measured and the baseline was corrected to fractions from untreated cells. Calibration curve was used to normalize results of fluorescence measurement. (B) Localization NF/pGL3 complexes in early endosomes (EE) and late endosomal, lysosomal compartments (LE). Cells were treated with complexes for 1 h followed by incubation in fresh media 0.5−4 h (chase time). The pGL3 Luc gene was amplified from all fractions positive for LAMP2 (LE, Lys) and Rab5 (EE) using PCR and visualized on 1% agarose gel. Relative fluorescence was measured and normalized as in (A).

utilize several pathways for internalization, such as clathrin and caveolae-mediated endocytosis and macropinocytosis.

Traffic of NF/pDNA Complexes along Endosomal Pathway. To gain better insight into the intracellular trafficking of NF/pDNA complexes, endosomal vesicles were purified using Percoll-based ultracentrifugation method. Percoll has been used to effectively separate different cell populations from tissues and organelles of cells.[34−36] We divided the separated material into 19 fractions and quantified DNA in each fraction with PCR. Based on the DNA content two distinct peaks were detected that corresponded to early endosomes and late endosomes/lysosomes containing fractions respectively, as verified by Western blot analysis using anti-Rab5 and anti-LAMP2 antibodies (data not shown).

NF51/pDNA complexes internalized the cells with high speed and efficacy (Figure 5A). Already in 10 min after treatment a small quantity of NF51 complexes was noticeable in endosomal vesicles, and in 30 min the amount of NF51 complexes in endosomal compartments surpassed the amount of NF1 complexes 2-fold. After a 4 h treatment period a 40% higher amount of NF51 complexes had internalized compared to the amount of NF1 complexes. Twenty-four hours after treatment almost no pDNA were detected in endosomal compartments delivered by either NF51 or NF1, suggesting that pDNA either is degraded or has escaped from endosomal compartments during that period of time. We conclude that larger amounts of NF51/pDNA complexes are internalized into HeLa cells and their internalization rate is also higher compared to NF1/pDNA nanoparticles.

To assess the further fate of internalized nanoparticles and their localization in early endosomal (EE) and late endosomal/lysosomal (LE) fractions, the treatment medium was removed after 1 h and the cells were incubated with fresh media for additional periods of time, named chase period (1 to 4 h), to let the complexes reach different endosomal compartments (Figure 5B). In 1 h after treatment nearly 2 times higher quantity of NF51 complexes was detected in EE, but at the same time the amount of NF1 complexes was higher in LE fractions. During the chase period the amount of NF51 and NF1 complexes in EE fractions decreased proportionally. After 4 h chase period the total amount of NF51 complexes that reached LE fractions was a little lower than the amount of NF1 complexes. We may hypothesize that although a totally higher amount of NF51/pDNA complexes enter endosomes, a significant part of them are released from early endosomal compartments and are not routed for degradation in lysosomes.

Analysis of pDNA/NF Nanocomplexes Internalization and Intracellular Localization by Electron Microscopy. In order to assess the internalization and intracellular targeting of NF1/pDNA and NF51/pDNA nanocomplexes in a more detailed manner we applied ultrastructural analysis using transmission electron microscopy (TEM). For the detection of pGL3 plasmid in TEM we tagged biotinylated pDNA first with about 2 gold clusters, using labeled neutravidin molecules, and then complexed with the respective peptide.

NF1/pDNA complexes associated with the plasma membrane as small clusters that contained 1−10 nanogold tags (black dots in Figure 6) implying the entrapment of 1−5 pDNA molecules in a nanoparticle. On the cell surface NF1/pDNA nanocomplexes were most often associated with membrane ruffles (Figure 6B) that in some cases had folded back and fused with the plasma membrane to form a macropinosome. In parallel with membrane ruffles, nanocomplexes were frequently detected in small (50−100 nm in diameter) membrane pits resembling caveolar invaginations (Figure 6A). After 1 h of incubation, part of the nanocomplexes had internalized and were detected in caveosomes and early endosomes. After longer incubation (4 h) the complexes were mostly targeted into multivesicular bodies (Figure 6E). Although the majority of nanoparticles remained entrapped in endosomal vesicles, a fraction of nanocomplexes had found a way to escape into cytosol (Figure 6E, inset).

NF51/pDNA nanocomplexes similarly to NF1/pDNA complexes were composed of 1−10 gold clusters at the cell surface (Figure 6C,D). These clusters were frequently

dx.doi.org/10.1021/bc4002757 | Bioconjugate Chem. 2013, 24, 1721−1732

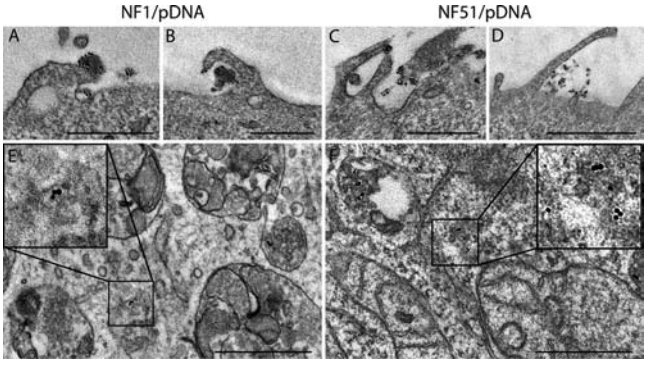

Figure 6. Uptake and intracellular localization of NF1/pDNA and NF51/pDNA nanocomplexes in HeLa cells. HeLa cells were incubated with preformed NF/pDNA complexes for 1−4 h at 37 °C. For the detection in transmission electron microscope pDNA was biotinylated and tagged with neutravidin-gold (black dots of 10 nm in figure) prior the experiment. On average 1−3 gold particles mark one pDNA molecule. (A−D) Interaction of NF1/pDNA (A, B) and NF51/pDNA (C,D) nanocomplexes with the cell surface after 1 h of incubation. (E,F) Localization of NF1/pDNA (E) and NF51/pDNA (F) in endosomal structures after 4 h of incubation. The insets in E and F represent magnified image of the boxed area of the same panel. Scale bars 500 nm; n, nucleus.

associated with membrane ruffles or localized in their close proximity. However, they did not induce the formation of caveolar invaginations or caveosomes, which was characteristic for NF1/pDNA complexes. One hour after the incubation, the nanocomplexes had internalized in the cells and were most often detected in multivesicular bodies. Some of the complexes had escaped the endosomes and were detected free in the cytosol. Four hours after the incubation the endocytic vesicles containing NF51/pDNA complexes were concentrated in the perinuclear region and about 1/10 th of nanocomplexes were located free in the cytosol (Figure 6F, inset).

Although both NF1/pDNA and NF51/pDNA complexes were often localized in the cytosol of HeLa cells, we could not detect these in nuclei after 4 h of incubation. This indicates that translocation into the nucleus is either a rare process or 4 h is not sufficient for the complexes to reach nucleus in amounts that are easily detected by TEM.

■ DISCUSSION

Cell-penetrating peptides are promising vectors for pDNA delivery, but their moderate transfection efficacy in the presence of serum has hindered their further development to clinical use. Unraveling the cellular uptake and intracellular trafficking mechanisms of cargo/transport vector complexes is highly important in order to harness their enormous therapeutic and diagnostic potential and to improve and to promote their *in vivo* applications. Extensive studies in the field of carrier vectors during the past decade have revealed that several factors, like the structure of the CPP, type of cargo, and how it is linked to the CPP (covalently or noncovalently) play an important role in the cellular uptake. In addition, several internalization routes may be active simultaneously.[5,6,11] The properties of the carrier vector have a huge impact on cell internalization, endosomal escape, and nuclear uptake of the cargo,[27] and an efficient carrier vector has to meet certain criteria.[3]

We have recently developed two novel cell-penetrating peptides that have proven their efficacy for the delivery of nucleic acids *in vitro*.[22,23] In the current work we studied in detail their complex formation with pDNA, uptake mechanism, intracellular trafficking, and endosomal escape for the further *in vivo* applications.

Gene-delivery vectors bind and condense pDNA into small, compact structures through electrostatic interactions between the negative phosphates of the DNA backbone and positive charges of the peptide, and also by hydrophobic interactions. The interactions between pDNA and transport vector should be balanced to offer protection from degradation as well as allow dissociation of the cargo after reaching the target in the nucleus or in the cytoplasm.[27] Dynamic light scattering demonstrated effective complexation of NickFects with pDNA (Table S1). NF1 and NF51 both condensed pDNA into small 60 nm size nanoparticles that in the presence of serum remained stable, despite increasing in size (Figure S1C) probably due to coating with salts and serum proteins. The surface charge of the nanoparticles in serum was negative (−9 to −11 mV). CD spectra showed like helixicity for both peptides complexed with pDNA (Figure S1A, B). However, heparin displacement assay uncovered differences in the properties of these nanoparticles (Figure 1A,B). NF51/pDNA complexes proved to be more resistant to heparin-induced decomplexation than NF1/pDNA nanoparticles. Relying on that, we may assume that NF1/pDNA complexes will release the cargo more easily while reaching the target.

To mimic the acidic conditions during the maturation process of endosomes and its impact on the stability of nanoparticles, we monitored the amount of intact NF/pDNA nanoparticles as a function of pH. NF51/pDNA complexes exposed relatively high stability to acidic environment, while NF1/pDNA complexes dissociated at pH 4.7 (Figure 1C). Confocal laser scanning microscopy also confirmed that NF51 has the tendency to form more homogeneous populations of complexes compared to NF1 and these complexes remain stable even 2 h after transfection (Figure 3A−D).

The initial step of internalization is the interaction of the nanoparticles with the plasma membrane. This may be driven by electrostatic forces between positively charged cationic CPPs and the negatively charged cell surface.[37] Membrane-associated proteoglycans, such as heparan sulfate proteoglycan, have been reported to play a crucial role in the cellular uptake of arginine-rich peptides like octa-Arginine and TAT.[38−40] DLS measurements of NF/pDNA complexes in serum-containing medium demonstrated the net negative surface charge of the nanoparticles. This excluded their interaction with negatively charged plasma membrane or integrated proteoglycans prior to cellular internalization due to repulsion. Recently we reported that the uptake of negatively charged CPP/cargo complexes is mediated by scavenger receptors.[24,31] Scavenger receptors are a family of cell surface glycoproteins that are known to bind promiscuously to polyanionic ligands and nanoparticles.[29,30] Scavenger receptors class A members, SCARA3 and SCARA5, played a crucial role in the uptake of stearylated TP10 analogue PepFect14/oligonucleotide complex.[31] In order to examine the role of SCARAs we tested the impact of inhibitory ligands, known to specifically bind to scavenger receptors, to the transfection efficacy of NF/pDNA nanoparticles. All used inhibitory ligands, e.g., poly I, dextransulfate, and fucoidin, reduced the biological activity of NF/pDNA complexes in a dose-dependent manner already at low concentrations (Figure 2A,B; Figure S3), and corroborated the involvement of scavenger receptors in the uptake of both

NF/pDNA complexes. Simultaneous down-regulation of SCARA3 and SCARA5 with siRNA led to more than 85% loss in the biological activity of both NF/pDNA complexes (Figure 2C,D) and proved that the above-mentioned receptors are highly engaged in the uptake of negatively charged NF/pDNA nanoparticles.

Upon membrane association, the nanoparticles are internalized from the cell exterior into the cytoplasm and endocytosis appears to be the predominant way of entry for most CPP/cargo complexes.[12] There is no specific method which could give an answer about the uptake mechanism and intracellular trafficking; therefore, a combination of different methods is required.[12] The energy-dependent uptake of NF/pDNA complexes was validated by lowering the temperature during transfection to 4 °C (Figure S4). Cotransfection with endosomolytic agent chloroquine (Figure 4A) confirmed the involvement of endocytotic vesicles, but indicated the exploitation of different endocytotic pathways by NF1 and NF51. Tracking of double-labeled peptide/pDNA complexes by confocal microscopy also revealed discrepancies in their uptake and intracellular trafficking (Figure 3), suggesting different endocytotic routes of internalization for NF51/pDNA and NF1/pDNA nanoparticles.

Pretreatment of cells with pharmacological inhibitors was used to reveal particular endocytotic pathways that were active in the uptake of NF/pDNA complexes. This is a widely used method, despite its drawbacks, e.g., lack of full specificity, and that the down-regulation of one pathway may up-regulate the other. Cytochalasine D, known as an inhibitor of macopinocytosis, reduced the biological activity of NF51/pDNA complex up to 25%, while chloropromazine and nystatin had no effect on transfection efficacy. NF1 mediated gene delivery was reduced more than 50% in the presence of both chloropromazine and cytochalasine D (Figure 4C,D), suggesting that NF1/pDNA nanoparticles utilize several pathways for internalization. According to this data we may speculate that NF51/pDNA nanoparticles are internalized preferentially via macropinocytosis whereas NF1/pDNA nanoparticles exploit clathrin- and caveolae-mediated endocytosis or macropinocytosis. To validate this, we followed the uptake and intracellular trafficking inside the cells on the ultracellular level. TEM revealed that NF51/pDNA particles formed larger conglomerates and associated with membrane ruffles, suggesting macropinocytosis as the route of entry, while NF1 in parallel formed smaller pits and induced less membrane ruffling (Figure 6).

Transmembrane scavenger receptors, which bind various anionic ligands, have been previously shown to utilize different endocytotic pathways. Several studies demonstrate that multiple pathways are active simultaneously and mediate the internalization of the nanoparticles into the cells. For example clathrin-dependent scavenger receptor A mediated endocytosis was found to be the major uptake mechanism for carboxy dextran-coated, negatively charged iron oxide nanoparticles in human macrophages. Nonetheless, the inhibition of macropinocytosis also had a slight, but significant impact on the uptake.[41] On the other hand, functionalized fullerene entered HEK cells using endocytotic pathway that exploits caveolae/lipid rafts and cytoskeletal components, and scavenger receptor inhibitior fucoidan completely blocked the uptake.[42] In addition, quantum dots with a carboxylic acid surface coating were recognized by lipid rafts but not by clathrin or caveolae in human epidermal keratinocytes and used endocytotic pathways that were primarily regulated by G-protein coupled receptors and scavenger receptors.[43]

Recently, it was reported that negatively charged silver nanoparticles in murine macrophage cells induced gradual clustering of the nanoparticles during the uptake and subsequent intracellular trafficking. Nanoparticles translocated into the cell interior through a vesicular trafficking process, but the intracellular distribution of nanoparticles varied significantly between individual cells. Application of various endocytosis inhibitors confirmed that the difference in intracellular nanoparticle organization resulted in actin- and clathrin-dependent endocytosis mechanisms. Furthermore, change in the spatial distribution of the nanoparticle agglomerates within the cells suggested some interplay of clathrin- and actin-based endocytosis machineries in the formation of agglomerates under inhibited conditions. The authors suggest that small nanoparticle clusters are taken up via clathrin-dependent but actin-independent pathway, whereas the other actin-dependent mechanism involves the association of nanoparticles into large clusters on the cell surface and these clusters are engulfed by actin-dependent pathway.[44]

Similarly, in our study TEM showed that NF51/pDNA complexes formed large conglomerates on the cell surface. These conglomerates associated with membrane ruffles or localized in their close proximity, referring to macropinocytosis as the way of entry. On the other hand, NF1/pDNA complexes associated with the plasma membrane as smaller clusters. They were frequently detected in close proximity to small membrane pits resembling caveolar invaginations, although they also associated with membrane ruffles (Figure 6). This is in compliance with data obtained from endocytosis inhibitors, referring to macropinocytosis as the major way of uptake for NF51/pDNA complexes, while NF1/pDNA complexes simultaneously utilized different endocytic pathways.

After budding from the plasma membrane the nanoparticles are confined in endocytotic vesicles. Sorting events initiated in EEs determine the subsequent fate of engulfed material. The vesicules trafficked through endolysosomal pathway experience gradual drop of pH in the vesicular environment and their content is finally targeted to lysosomes for degradation.[32] So, the next barrier for CPP/cargo nanoparticles to overcome for reaching the site of action is endosomal release. Quantitative comparison of intracellular trafficking is important for clarification of which intracellular process is responsible for certain transfection efficacy.[45] However, the fate of the complexes after cell entry has been less investigated and very little information exists on their intracellular trafficking.[11]

The Percoll-based ultracentrifugation method has been used to effectively separate different cell populations from tissues and organelles from cells,[34−36] but to our knowledge this is the first time the Percoll gradient was used to extract and study CPP/cargo complexes in endosomal vesicles. We separated DNA fractions at different time points of internalization and quantified the content of DNA by PCR. Totally, a larger amount of NF51/pDNA complexes internalized into HeLa cells and the internalization rate was higher compared to NF1/pDNA complexes. It is noteworthy that a relatively small amount of NF51/pDNA nanoparticles reached late endosomal/lysosomal compartments (Figure 5). We may presume that, although NF51/pDNA complexes enter EE-like vesicles, a substantial amount is able to escape from early endosomal compartments and is not routed for degradation in lysosomes. These results are in accordance with transfection experiments

in the presence of chloroquine (Figure 4A) and our earlier results from protein transduction by TP10.[32] CQ is known to accumulate in late endosomes/lysosomes, buffer the pH there, and induce osmotic swelling of the vesicles. This results in the destabilization of the endosomal membrane and release of the nanoparticles. Cotreatment with CQ evidenced the entrapment of NF1/pDNA complexes in endosomal compartments. However, destabilization of endosomes revealed no positive effect on NF51 mediated transfection. So we may suggest that NF51 itself is capable of disrupting the endosome membrane and promoting endosomal escape of the nanoparticles.

Real-time imaging of labeled NF/pDNA complex internalization to HeLa cells using confocal microscopy also showed dissimilarities in NF/pDNA complex trafficking. NF51/pDNA complexes retained their yellowish color even after 2 h of incubation, whereas NF1/pDNA complexes turned red (Figure 3). The loss of green fluorescence signal is probably the result of partial dissociation of NF1 from complex with pDNA. It also indicates to the pH drop during the maturation of early endosomes into late endosomes and the quenching of fluorescein emission at acidic pH that also leads to decrease of green color. These results are also in accordance with DLS measurements where we followed NF/pDNA complex stability at different pH values (Figure 1C).

Molecules entering by clathrin mediated endocytic pathway experience a drop in pH from neutral to pH 5.9 in early endosomes, with further reduction to pH 5 in lysosomes. In comparison to rapid and dynamic clathrin-medited endocytosis, caveolae-mediated endocytosis is slow. Although caveolar uptake is a nonacidic route of internalization, the small vesicles slowly carry little fluid phase volume. Thus, it is unlikely that this process contributes significantly to the uptake of NF/pDNA nanoparticles.[46]

According to our data, it is reasonable to suggest that NF1/pDNA complexes that utilize clathrin-mediated pathway are trapped in endocytic vesicles and experience a drop of pH due to fusion of early endosomes with late endosomes/lysosomes. Cotransfection with chloroquine promotes their release from late endosomal/lysosomal compartments and so enhances the transfection efficacy.

NF51/pDNA complexes are internalized predominantly via macropinocytosis. Although the pH of macropinosomes decreases, they do not fuse into lysosomes.[46] Macropinosomes are thought to be inherently leaky vesicles compared with other types of endosomes[47] and NF51/pDNA complexes are able to break loose from there. Due to the fact, chloroquine, which destabilizes the membranes of the lysosomes, has only a minor impact on pDNA transfection with NF51. For drug delivery macropinocytosis provides several advantageous aspects: large volume of solution is taken up, the lysosomal degradation is avoided or postponed, and macropinosomes are of relatively leaky nature, which enables endosomal escape.

Considering all our results, we may suggest that we are dealing with two limiting processes in parallel. NF51 and NF1 complexes with pDNA are passing two different bottlenecks in order to induce efficient gene expression. NF51/pDNA complexes enter the cells rapidly, in high amounts, and they are able to escape from endosomes, but NF51 condenses pDNA into tight nanoparticles and hampers pDNA unpacking. On the other hand, a higher amount of NF1/pDNA complexes is entrapped in endosomes. However, these nanoparticles are more loosely packed and pDNA can dissociate from the complex. As a result of these two limiting processes the gene transfection mediated by NF51 or NF1 is on quite the same level.

Extensive studies with a variety of nonviral vectors have specified the requirements for an ideal transport vector.[14,27] The current study points out several of them, like interaction between delivery vector and pDNA, particle size and surface charge, cellular internalization and intracellular trafficking, endosomal escape, and dissociation of the cargo from the nanoparticles before the site of action. Furthermore, the extraction and study of endosomal compartments, and new method to examine CPP/cargo complex intracellular trafficking proved to be highly lucrative and provided valuable quantifiable information about endosomal escape.

Taken together, NickFects are highly potent transport vectors for pDNA delivery both for *in vitro* and *in vivo* applications. They condense pDNA into small nanoparticles with negative surface charge, but NF1/pDNA nanoparticles are less stable in acidic environment and to the displacement with heparin. NF/pDNA nanoparticles interact with cell surface through SCARA3 and SCARA5 receptors and exploit different endocytotic pathways for internalization. NF51/pDNA complexes enter via macropinocytosis, while NF1/pDNA nanoparticles use clathrin-mediated endocytosis and macropinocytosis. Importantly, NF51 nanoparticles are able to promote better endosomal escape than NF1/pDNA nanoparticles.

In conclusion, we have developed two highly efficient transport vectors for pDNA, although these vectors have radically different modifications in the backbone. The data presented in the current work suggest that the transfection efficacy of NF1 and NF51 is achieved by using differential transfection pathways. Unraveling the uptake mechanism and intracellular trafficking of NF/pDNA nanoparticles provided us with valuable data for their further *in vivo* applications. Furthermore, we discovered that NF1 and NF51 have different bottlenecks for achieving highly effective pDNA transfection and this enables further development of these vectors in order to achieve higher bioavailability of macromolecule-based drugs.

■ ASSOCIATED CONTENT

Supporting Information

Scheme S1: Chemical structures of NF51 and NF1. (Stearyl is CH_3-(CH_2)16-CO−). Table S1: Average diameter, Zeta potential and PdI of NickFect/pDNA nanoparticles determined by DLS measurements Figure S1: CD spectra of NF and NF/pDNA complexes in water. Stability of NF/pDNA complexes in serum. Figure S2: Plasmid transfection efficacy of NickFects in HeLa cells. Figure S3: Scavenger receptor inhibition with specific ligands suppresses the activity of NF51/pDNA and NF1/pGL3 complexes. Figure S4: Effect of lowered temperature on pDNA transfection mediated by NF51 and NF1 in HeLa cells in serum containing medium. This material is available free of charge via the Internet at http://pubs.acs.org.

■ AUTHOR INFORMATION

Corresponding Author

*E-mail: piret.arukuusk@ut.ee. Phone: +372-7-37-4867; Fax: +372-7-37-4900.

Notes

The authors declare no competing financial interest.

■ ACKNOWLEDGMENTS

The work was supported by the EU through Centre of Excellence of Chemical Biology, SF0180027s08, SF0180019s11, ETF9438, project HCV-Tech (3.2.0701.11-0015), by the Swedish Research Council (VRNT) and Cepep AB. We kindly thank Nikita Oskolkov for his brilliant ideas and for reading the manuscript. We also thank Dana Maria Copolovici for her help and Kariem Ezzat for fruitful discussions. We also thank Ago Rinken and Sergei Kopanchuk for the opportunity to use and for the assistance with TIRF microscopy.

■ ABBREVIATIONS

EDTA, ethylenediaminetetraacetic acid; CPP, cell-penetrating peptide; CR, charge ratio; DLS, dynamic light scattering; HOBt, hydroxybenzotrazole; HBTU, *O*-Benzotriazole-*N*,*N*,*N*^{0},*N*^{0}-tetramethyluronium-hexafluoro-phosphate; DIEA, diisopropylethylamine; NF, NickFect; pGL3, luciferase expressing plasmid; TAE, tris-acetate-EDTA; TEM, transmission electron microscopy; TFA, trifluoroacetic acid; TIS, triisopropylsilane

■ REFERENCES

(1) Kay, M. A. (2011) State-of-the-art gene-based therapies: the road ahead. *Nat. Rev. Genet. 12*, 316−28.

(2) Glover, D. J., Lipps, H. J., and Jans, D. A. (2005) Towards safe, non-viral therapeutic gene expression in humans. *Nat. Rev. Genet. 6*, 299−310.

(3) Pack, D. W., Hoffman, A. S., Pun, S., and Stayton, P. S. (2005) Design and development of polymers for gene delivery. *Nat. Rev. Drug Discovery 4*, 581−93.

(4) Heitz, F., Morris, M. C., and Divita, G. (2009) Twenty years of cell-penetrating peptides: from molecular mechanisms to therapeutics. *Br. J. Pharmacol. 157*, 195−206.

(5) Järver, P., Mäger, I., and Langel, Ü. (2010) In vivo biodistribution and efficacy of peptide mediated delivery. *Trends Pharmacol. Sci. 31*, 528−35.

(6) Said Hassane, F., Saleh, A. F., Abes, R., Gait, M. J., and Lebleu, B. (2010) Cell penetrating peptides: overview and applications to the delivery of oligonucleotides. *Cell. Mol. Life Sci. 67*, 715−26.

(7) Brasseur, R., and Divita, G. (2010) Happy birthday cell penetrating peptides: already 20 years. *Biochim. Biophys. Acta 1798*, 2177−81.

(8) Hoyer, J., and Neundorf, I. (2012) Peptide vectors for the nonviral delivery of nucleic acids. *Acc. Chem. Res. 45*, 1048−56.

(9) Koren, E., and Torchilin, V. P. (2012) Cell-penetrating peptides: breaking through to the other side. *Trends Mol. Med. 18*, 385−93.

(10) Vasconcelos, L., Pärn, K., and Langel, Ü. (2013) THerapeutic potential of cell-penetrating peptides. *Ther. Delivery 4*, 1−.

(11) Räägel, H., Säälik, P., and Pooga, M. (2010) Peptide-mediated protein delivery-which pathways are penetrable? *Biochim. Biophys. Acta 1798*, 2240−8.

(12) Madani, F., Lindberg, S., Langel, Ü., Futaki, S., and Gräslund, A. (2011) Mechanisms of cellular uptake of cell-penetrating peptides. *J. Biophys. 2011*, 414729.

(13) Duchardt, F., Fotin-Mleczek, M., Schwarz, H., Fischer, R., and Brock, R. (2007) A comprehensive model for the cellular uptake of cationic cell-penetrating peptides. *Traffic 8*, 848−66.

(14) Lehto, T., Kurrikoff, K., and Langel, Ü. (2012) Cell-penetrating peptides for the delivery of nucleic acids. *Expert Opin. Drug Delivery 9*, 823−36.

(15) Rydström, A., Deshayes, S., Konate, K., Crombez, L., Padari, K., Boukhaddaoui, H., Aldrian, G., Pooga, M., and Divita, G. (2011) Direct translocation as major cellular uptake for CADY self-assembling peptide-based nanoparticles. *PLoS One 6*, e25924.

(16) Deshayes, S., Konate, K., Aldrian, G., Crombez, L., Heitz, F., and Divita, G. (2010) Structural polymorphism of non-covalent peptide-based delivery systems: highway to cellular uptake. *Biochim. Biophys. Acta 1798*, 2304−14.

(17) Khalil, I. A., Kogure, K., Futaki, S., Hama, S., Akita, H., Ueno, M., Kishida, H., Kudoh, M., Mishina, Y., Kataoka, K., Yamada, M., and Harashima, H. (2007) Octaarginine-modified multifunctional envelope-type nanoparticles for gene delivery. *Gene Ther. 14*, 682−9.

(18) Lo, S. L., and Wang, S. (2008) An endosomolytic Tat peptide produced by incorporation of histidine and cysteine residues as a nonviral vector for DNA transfection. *Biomaterials 29*, 2408−14.

(19) El Andaloussi, S., Lehto, T., Mäger, I., Rosenthal-Aizman, K., Oprea, I. I., Simonson, O. E., Sork, H., Ezzat, K., Copolovici, D. M., Kurrikoff, K., Viola, J. R., Zaghloul, E. M., Sillard, R., Johansson, H. J., Said Hassane, F., Guterstam, P., Suhorutsenko, J., Moreno, P. M., Oskolkov, N., Halldin, J., Tedebark, U., Metspalu, A., Lebleu, B., Lehtio, J., Smith, C. I., and Langel, Ü. (2011) Design of a peptide-based vector, PepFect6, for efficient delivery of siRNA in cell culture and systemically in vivo. *Nucleic Acids Res. 39*, 3972−3987.

(20) Khalil, I. A., Futaki, S., Niwa, M., Baba, Y., Kaji, N., Kamiya, H., and Harashima, H. (2004) Mechanism of improved gene transfer by the N-terminal stearylation of octaarginine: enhanced cellular association by hydrophobic core formation. *Gene Ther. 11*, 636−44.

(21) Mäe, M., El Andaloussi, S., Lundin, P., Oskolkov, N., Johansson, H. J., Guterstam, P., and Langel, Ü. (2009) A stearylated CPP for delivery of splice correcting oligonucleotides using a non-covalent co-incubation strategy. *J. Controlled Release 134*, 221−227.

(22) Oskolkov, N., Arukuusk, P., Copolovici, D. M., Lindberg, S., Margus, H., Padari, K., Pooga, M., and Langel, Ü. (2011) NickFects, Phosphorylated Derivatives of Transportan 10 for Cellular Delivery of Oligonucleotides. *Int. J. Pept. Res. Ther. 17*, 147−157.

(23) Arukuusk, P., Pärnaste, L., Oskolkov, N., Copolovici, D. M., Margus, H., Padari, K., Möll, K., Maslovskaja, J., Tegova, R., Kivi, G., Tover, A., Pooga, M., Ustav, M., and Langel, Ü. (2013) New generation of efficient peptide-based vectors, NickFects, for the delivery of nucleic acids. *Biochim. Biophys. Acta 1828*, 1365−73.

(24) Säälik, P., Padari, K., Niinep, A., Loorents, A., Hansen, M., Jokitalo, E., Langel, Ü., and Pooga, M. (2009) Protein delivery with transportans is mediated by caveolae rather than flotillin-dependent pathways. *Bioconjugate Chem. 20*, 877−87.

(25) Zhang, S., Li, J., Lykotrafitis, G., Bao, G., and Suresh, S. (2009) Size-Dependent Endocytosis of Nanoparticles. *Adv. Mater. 21*, 419−424.

(26) Maeda, H. (2010) Tumor-selective delivery of macromolecular drugs via the EPR effect: background and future prospects. *Bioconjugate Chem. 21*, 797−802.

(27) Viola, J. R., El-Andaloussi, S., Oprea, I. I., and Smith, C. I. (2010) Non-viral nanovectors for gene delivery: factors that govern successful therapeutics. *Expert Opin. Drug Delivery 7*, 721−35.

(28) Veiman, K. L., Mäger, I., Ezzat, K., Margus, H., Lehto, T., Langel, K., Kurrikoff, K., Arukuusk, P., Suhorutsenko, J., Padari, K., Pooga, M., Lehto, T., and Langel, Ü. (2012) PepFect14 peptide vector for efficient gene delivery in cell cultures. *Mol. Pharmacol. 10*, 199−210.

(29) Platt, N., and Gordon, S. (1998) Scavenger receptors: diverse activities and promiscuous binding of polyanionic ligands. *Chem. Biol. 5*, R193−203.

(30) Peiser, L., and Gordon, S. (2001) The function of scavenger receptors expressed by macrophages and their role in the regulation of inflammation. *Microbes Infect. 3*, 149−59.

(31) Ezzat, K., Helmfors, H., Tudoran, O., Juks, C., Lindberg, S., Padari, K., El-Andaloussi, S., Pooga, M., and Langel, U. (2012) Scavenger receptor-mediated uptake of cell-penetrating peptide nanocomplexes with oligonucleotides. *Faseb J. 26*, 1172−80.

(32) Räägel, H., Säälik, P., Hansen, M., Langel, Ü., and Pooga, M. (2009) CPP-protein constructs induce a population of non-acidic vesicles during trafficking through endo-lysosomal pathway. *J. Controlled Release 139*, 108−17.

(33) Langel, Ü. (2006) *Cell-penetrating Peptides: Process and Applications*, 2nd ed., CRC Press, Boca Raton.
(34) Campanella, M., Sciorati, C., Tarozzo, G., and Beltramo, M. (2002) Flow cytometric analysis of inflammatory cells in ischemic rat brain. *Stroke 33*, 586−92.
(35) Jouret, F., Courtoy, P. J., and Devuyst, O. (2011) Segmental and subcellular distribution of CFTR in the kidney. *Methods Mol. Biol. 741*, 285−99.
(36) Gao, J., Xia, L., Lu, M., Zhang, B., Chen, Y., Xu, R., and Wang, L. (2012) TM7SF1 (GPR137B): a novel lysosome integral membrane protein. *Mol. Biol. Rep. 39*, 8883−9.
(37) Nakase, I., Akita, H., Kogure, K., Gräslund, A., Langel, Ü., Harashima, H., and Futaki, S. (2011) Efficient intracellular delivery of nucleic acid pharmaceuticals using cell-penetrating peptides. *Acc. Chem. Res. 45*, 1132−9.
(38) Gump, J. M., and Dowdy, S. F. (2007) TAT transduction: the molecular mechanism and therapeutic prospects. *Trends Mol. Med. 13*, 443−8.
(39) Nakase, I., Niwa, M., Takeuchi, T., Sonomura, K., Kawabata, N., Koike, Y., Takehashi, M., Tanaka, S., Ueda, K., Simpson, J. C., Jones, A. T., Sugiura, Y., and Futaki, S. (2004) Cellular uptake of arginine-rich peptides: roles for macropinocytosis and actin rearrangement. *Mol. Ther. 10*, 1011−22.
(40) Imamura, J., Suzuki, Y., Gonda, K., Roy, C. N., Gatanaga, H., Ohuchi, N., and Higuchi, H. (2011) Single particle tracking confirms that multivalent Tat protein transduction domain-induced heparan sulfate proteoglycan cross-linkage activates Rac1 for internalization. *J. Biol. Chem. 286*, 10581−92.
(41) Lunov, O., Zablotskii, V., Syrovets, T., Rocker, C., Tron, K., Nienhaus, G. U., and Simmet, T. (2010) Modeling receptor-mediated endocytosis of polymer-functionalized iron oxide nanoparticles by human macrophages. *Biomaterials 32*, 547−55.
(42) Zhang, L. W., Yang, J., Barron, A. R., and Monteiro-Riviere, N. A. (2009) Endocytic mechanisms and toxicity of a functionalized fullerene in human cells. *Toxicol. Lett. 191*, 149−57.
(43) Zhang, L. W., and Monteiro-Riviere, N. A. (2009) Mechanisms of quantum dot nanoparticle cellular uptake. *Toxicol. Sci. 110*, 138−55.
(44) Wang, H., Wu, L., and Reinhard, B. M. (2012) Scavenger receptor mediated endocytosis of silver nanoparticles into J774A.1 macrophages is heterogeneous. *ACS Nano 6*, 7122−32.
(45) Akita, H., and Harashima, H. (2008) Advances in non-viral gene delivery: using multifunctional envelope-type nano-device. *Expert Opin. Drug Delivery 5*, 847−59.
(46) Khalil, I. A., Kogure, K., Akita, H., and Harashima, H. (2006) Uptake pathways and subsequent intracellular trafficking in nonviral gene delivery. *Pharmacol. Rev. 58*, 32−45.
(47) Wadia, J. S., Stan, R. V., and Dowdy, S. F. (2004) Transducible TAT-HA fusogenic peptide enhances escape of TAT-fusion proteins after lipid raft macropinocytosis. *Nat. Med. 10*, 310−5.